

# Antiferromagnetism, charge density wave, and $d$ -wave superconductivity in the $t$ - $J$ - $U$ - $V$ model of correlated electrons: Role of direct Coulomb interactions

Marcin Abram,<sup>1,\*</sup> Michał Zegrodnik,<sup>2,†</sup> and Józef Spałek<sup>1,‡</sup>

<sup>1</sup>*Marian Smoluchowski Institute of Physics, Jagiellonian University, Łojasiewicza 11, 30-348 Kraków, Poland*

<sup>2</sup>*Academic Centre for Materials and Nanotechnology,*

*AGH University of Science and Technology, Al. Mickiewicza 30, 30-059 Kraków, Poland*

(Dated: August 4, 2016)

We study the stability of antiferromagnetic (AF), charge density wave (CDW), and superconducting (SC) states within the  $t$ - $J$ - $U$ - $V$  model of strongly correlated electrons using the statistically consistent Gutzwiller approximation (SGA). We concentrate on the role of the intersite Coulomb interaction term  $V$  in stabilizing the CDW phase and show it appears only above some critical values of  $V$  and in a limited hole doping range  $\delta$ . The effect of the term  $V$  on SC and AF phases is that a strong interaction suppresses SC altogether, whereas the AF order is not significantly influenced by its presence. Calculations for the case of pure SC phase have been also carried out within an extended approach, the diagrammatic expansion for the Gutzwiller wave function (DE-GWF) in order to analyze influence of the higher-order correlations onto this phase beyond the renormalized mean field approach. In the Appendices we discuss, the specific ambiguity of the choice of the Gutzwiller renormalization factors within the SGA when either AF or CDW orders are considered.

PACS numbers: 71.45.Lr, 71.10.Fd, 71.10.-w

## I. INTRODUCTION

Charge ordering (CO) was observed for the first time in 1939 in  $\text{Fe}_3\text{O}_4$  [1, 2] and since then, it has been commonly seen in electronically correlated transition metal oxides [3]. The interest in this field grew again recently after the discovery of the charge density wave (CDW) state in cuprate high temperature superconductors for underdoped samples [3–5] (cf. Fig. 1 for reference). In effect, an ample evidence has accumulated about the role played by the CDW instability in the copper based materials [3, 6–11]. It has also been suggested that for certain materials the CDW state may have a three-dimensional character in nonzero magnetic field [12, 13]. It was also argued, that the CDW order parameter may have a  $d$ -wave symmetry [14–16], and that there is a connection between the pseudogap phase appearance in the cuprates and the charge ordering [9, 17, 18]. Regarding theoretical analysis, various calculation schemes have been applied to the (extended) Hubbard and  $t$ - $J$  models to investigate the stability of CO states [16, 19–22]. In this respect, the appearance of the so-called pair-density-wave state has been proposed which can coexist with CDW state and lead to the appearance of the pseudogap anomaly [23, 24]. Finally, it has been implied very recently [25] that the CDW solution for the  $t$ - $J$  model has always a slightly higher energy than the generic SC+AF solution. All of this evidence means that a further analysis of

CDW instability in the  $t$ - $J$  and related models is required to verify if the widely used methods of approach to this phenomena can yield a convergent description of unconventional phases in the copper based materials and to what extent they cooperate or compete with each other in those quasi-two-dimensional strongly correlated materials.

Encouraged by our recent results obtained within the  $t$ - $J$ - $U$  model [26, 27], which match well with experimental results for the cuprates, we concentrate here on the role of intersite Coulomb repulsion within the  $t$ - $J$ - $U$ - $V$  model. In such a picture the intraatomic (Hubbard) interaction magnitude  $U$  is not regarded as extremely strong which means that the limit  $U/t \rightarrow \infty$  is not assumed. In this situation, a straightforward decomposition of the narrow-band states into the Hubbard subbands, with the upper subband (for the band filling  $n \leq 1$ ) being unoccupied, is not physically realized and the  $t$ - $J$  model does not follow directly from the perturbation expansion of the Hubbard model in powers of  $t/U$ . Instead, the antiferromagnetic kinetic exchange interaction arises from the superexchange via  $2p_\sigma$  states due to oxygen [28]. Consequently, nonzero double occupancies are allowed for a non-half-filled band case and in such a situation the Hubbard term  $\sim U$  provides a direct contribution to the states. This argument justifies the generalization of the  $t$ - $J$  model to the  $t$ - $J$ - $U$  form. The additional term  $\sim V$  is added here to analyze its importance for the CDW state stability [29]. Originally, the Hubbard term has been added to the  $t$ - $J$  model when introducing the so-called Gossamer superconductivity (for detailed discussion cf. Ref. [26] and papers cited therein; cf. also Refs. [30, 31]).

In our analysis we consider the three most impor-

\* abram.mj@gmail.com

† michal.zegrodnik@agh.edu.pl

‡ ufspalek@if.uj.edu.pl

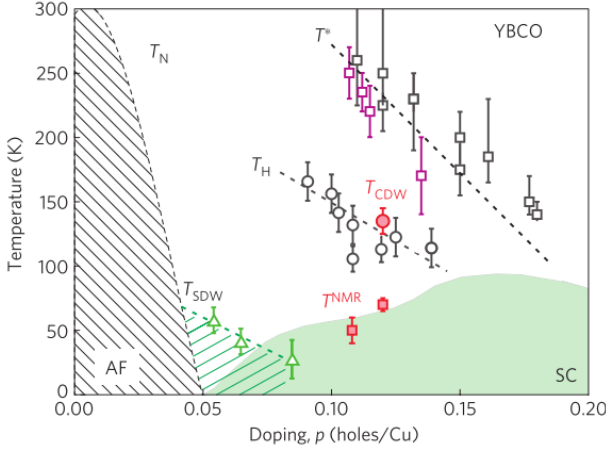


Figure 1. (Color online) Experimental phase diagram of  $\text{YBa}_2\text{Cu}_3\text{O}_{6+x}$  (YBCO) on hole-doping–temperature plane. The shaded regions represent the superconducting (SC) and antiferromagnetic (AF) phases (with the Néel temperature  $T_N$ ), as well as the region where the spin-density-wave (SDW) state is observed. Note, that the CDW critical temperature  $T_{CDW}$  is about twice larger than the critical temperature of SC phase. The pseudogap is marked by  $T^*$  (black squares represent the Nernst effect measurements, and the purple squares the neutron diffraction). Finally,  $T_H$  stands for the critical temperature of the large and negative Hall effect, while  $T^{NMR}$  for the temperature scale, below which the field-induced charge order is observed using NMR (Figure taken from Ref. [9]).

tant phases related to the cooper-based high temperature superconducting (HTS) compounds: antiferromagnetic (AF), charge ordered (CDW), and superconducting (SC) phases. We show first that the presence of the  $V$  term is necessary for CDW stability.

In the first part of this paper, the analysis is carried out with the use of the *statistically consistent Gutzwiller approximation* (SGA), within which we can account for correlation effects in a reasonable computing time (cf. derivation of SGA method in Refs. [32, 33] and its various applications in Refs. [26, 34]). In the second part of the paper (cf. Sec. IV B), we test the robustness of the pure superconducting solution beyond SGA, i.e., using a *systematic diagrammatic expansion of the Gutzwiller-wave function* (DE-GWF method). This last approach allows us to go beyond the SGA in a systematic manner and to take into account, in higher orders, the non-local correlations of the increased range in space. The differences between the SGA and the DE-GWF solutions are specified there. Additionally, in the Appendix A, we discuss an inherent ambiguity in choosing the Gutzwiller renormalization factors when either AF or CDW states are considered in SGA. Namely, we show that different calculation schemes used in the literature lead also to different forms of the Gutzwiller factors, what results in

different stability regimes of the AF phase.

## II. $t$ - $J$ - $U$ - $V$ MODEL

The starting Hamiltonian for the subsequent analysis has the form,

$$\begin{aligned} \hat{\mathcal{H}}_{t-J-U-V} = & t \sum_{\langle i,j \rangle, \sigma} (\hat{c}_{i\sigma}^\dagger \hat{c}_{j\sigma} + H.c.) + t' \sum_{\langle\langle i,j \rangle\rangle, \sigma} (\hat{c}_{i\sigma}^\dagger \hat{c}_{j\sigma} + H.c.) \\ & + J \sum_{\langle i,j \rangle} \hat{\mathbf{S}}_i \cdot \hat{\mathbf{S}}_j + U \sum_i \hat{n}_{i\uparrow} \hat{n}_{i\downarrow} + \underbrace{\left( \tilde{V} - \frac{1}{4} J \right)}_V \sum_{\langle i,j \rangle, \sigma, \sigma'} \hat{n}_{i\sigma} \hat{n}_{j\sigma'}, \end{aligned} \quad (1)$$

where  $\sum_{\langle i,j \rangle}$  and  $\sum_{\langle\langle i,j \rangle\rangle}$  denote summation over all nearest and second nearest neighbors, respectively, with each pair being counted only once, i.e., when pair  $(i, j)$  is counted, then  $(j, i)$  is not. Furthermore,  $t$  and  $t'$  are respectively the hopping amplitudes between the nearest and the next nearest neighboring sites,  $J$  is the antiferromagnetic exchange integral, and  $U$  ( $\tilde{V}$ ) is the onsite (intersite) Coulomb repulsion magnitude. The standard notation is used, where  $\hat{c}_{i\sigma}^\dagger$  and  $\hat{c}_{i\sigma}$  are, respectively, the creation and the annihilation operators, for electron with spin quantum number  $\sigma = \pm 1$  located at site  $i$ . Similarly,  $\hat{n}_{i\sigma} \equiv \hat{c}_{i\sigma}^\dagger \hat{c}_{i\sigma}$  and  $\hat{\mathbf{S}}_i \equiv (\hat{S}_i^+, \hat{S}_i^-, \hat{S}_i^z)$ , where  $\hat{S}_i^+ \equiv \hat{c}_{i\sigma}^\dagger \hat{c}_{i\bar{\sigma}}$ , and  $\hat{S}_i^z \equiv \frac{1}{2} (\hat{n}_{i\uparrow} - \hat{n}_{i\downarrow})$ .

As has already been mentioned, the appearance of the  $J$  term in this approach is attributed mainly to the  $d$ - $d$  superexchange via  $2p_\sigma$  states due to oxygen [28]. The finite value of the Coulomb repulsion  $U$  leads to a relatively small but nonzero population of the upper Hubbard subband [30, 31, 35]. In such a situation the appearance of both the  $J$  and the  $U$  terms is physically admissible in the Hamiltonian. For  $V = 0$  and when  $U \rightarrow \infty$ , the limit of the  $t$ - $J$  model is recovered. On the other hand, for  $J = V = 0$ , we obtain the limit of the Hubbard model. Nevertheless, our model is not only constructed as a formal generalization of the two limits. As can be seen from the numerous estimates of the model parameters, the typical values of the parameters of the one-band model are:  $t = -0.35$  eV, and  $U \approx 8$ –10 eV, so that the ratio of  $U$  to the bare bandwidth  $W = 8|t|$  is  $U/W \approx 2.5$ –3, i.e., only by the factor of about two higher than typical required for Mott-Hubbard localization [36]. As a consequence, the Hubbard gap is  $U - W \sim W$  and the double occupancy can be estimated as  $d^2 \sim \frac{t}{U} \delta \sim 10^{-2}$ , where  $\delta$  is the hole doping. Additionally, the value of  $U$  is reduced to the value  $U - V \sim \frac{2}{3}U$  when the  $V$  term is present [37]. Also, as said above, the value of  $J$  cannot be regarded as resulting from the  $t/U$  expansion of the (extended) Hubbard model [37–43], and both  $J$  and  $U$  can be treated as independent variables. The last term comes partially from the derivation of  $t$ - $J$  model from the Hubbard model (cf. [37–39, 41–44]) and

partially (the part  $\sim \tilde{V}$ ) represents an explicit intersite Coulomb repulsion of electrons located on the nearest neighboring sites. For simplicity, we denote  $V \equiv \tilde{V} - \frac{1}{4}J$ .

### III. METHODS

#### A. Statistically Consistent Gutzwiller Approximation (SGA)

To solve the Hamiltonian (1), we first use the statistically consistent Gutzwiller approximation (SGA) [32, 33, 45, 46]). The main idea behind the Gutzwiller approach is to express the wave function of the system in the following form

$$|\Psi\rangle = \hat{P}|\Psi_0\rangle \equiv \prod_{\mathbf{k}} \hat{P}_i |\Psi_0\rangle, \quad (2)$$

where the correlator  $\hat{P}_i$  weights the configuration of given local occupancies (0,  $\uparrow$ ,  $\downarrow$ ,  $\uparrow\downarrow$ ) and  $|\Psi_0\rangle$  is the non-correlated single particle wave function, generally assumed in the broken-symmetry state of our choice. In such a situation, the expectation value of the ground-state energy of the system can be expressed as follows,

$$E = \frac{\langle \Psi | \hat{H} | \Psi \rangle}{\langle \Psi | \Psi \rangle} = \frac{\langle \Psi_0 | \hat{P} \hat{H} \hat{P} | \Psi_0 \rangle}{\langle \Psi_0 | \hat{P}^2 | \Psi_0 \rangle} \approx \langle \Psi_0 | \hat{H}_{eff} | \Psi_0 \rangle. \quad (3)$$

In other words, instead of calculating the average of the initial Hamiltonian (1) with respect to usually complicated, many-particle, wave function  $|\Psi\rangle$ , we choose to modify that Hamiltonian (presumably by making it more complicated) in order to have the relatively simple task of calculating its average with respect to the wave function  $|\Psi_0\rangle$  represented by a single Slater determinant. In our case, the resultant expectation value is depended on many quantities,

$$\langle \Psi_0 | \hat{H}_{t-J-U-V}^{eff} | \Psi_0 \rangle \equiv W(n, m, \delta_n, d_A, d_B, \chi, \chi_S, \chi_T, \Delta_S, \Delta_T), \quad (4)$$

where  $W(\dots)$  is a functional of a number of mean-field averages that are explained below (for the explicit form of  $W$  and the details of the calculations see Appendix A). First,  $n$  is the average number of electrons per site,  $m$  is the magnitude of staggered magnetization in AF state, and  $\delta_n$  is the order parameter for CDW phase. Those three quantities can be combined together by expressing the local occupancy in the following manner,

$$n_{i\sigma} \equiv \langle \hat{c}_{i\sigma}^\dagger \hat{c}_{i\sigma} \rangle_0 \equiv \frac{1}{2} (n + e^{i\mathbf{Q}\cdot\mathbf{R}_i} (\sigma m + \delta_n)), \quad (5)$$

where for simplicity, we denote  $\langle \Psi_0 | \dots | \Psi_0 \rangle \equiv \langle \dots \rangle_0$ . The superlattice vector was first chosen to be  $\mathbf{Q} = (\pi, \pi)$ , i.e., the lattice is naturally divided into two sublattices,

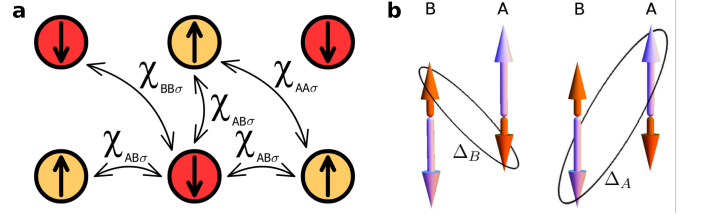


Figure 2. (Color online) Schematic interpretation of  $\chi_{AB\sigma} \equiv \chi_{\sigma}$ ,  $\chi_{AA\sigma}$  and  $\chi_{BB\sigma}$  (panel a) and  $\Delta_A$  and  $\Delta_B$  (panel b). To include antiferromagnetic ordering we divide the lattice into two sublattices, A where in majority spins are  $up$ , and B where there are  $down$ . Thus,  $\chi_{AB\sigma}$  denotes hopping of  $\sigma$  electron between the sublattices A and B, while  $\chi_{AA\sigma}$  and  $\chi_{BB\sigma}$  the hopping within one sublattice (A or B respectively);  $\Delta_A$  denotes the pairing amplitude of majority spins  $up$  from sublattice A and minority spins  $down$  from B, and  $\Delta_B$  pairing of majority spins  $up$  from B and minority spins  $down$  from A. Additionally, if CDW is present, then for site belonging to the A sublattice the average (total) number of electrons should be larger by  $\delta_n$ , with respect to the neighboring site belonging to the B sublattice (for clarity, in this picture it was assumed that  $\delta_n = 0$ ).

A and B, such that one sublattice (A) has in average  $\frac{1}{2}(n + m + \delta_n)$   $up$  ( $\uparrow$ ) electrons and  $\frac{1}{2}(n - m + \delta_n)$   $down$  ( $\downarrow$ ) electrons, while the second sublattice (B) has in average  $\frac{1}{2}(n - m - \delta_n)$   $up$  ( $\uparrow$ ) and  $\frac{1}{2}(n + m - \delta_n)$   $down$  ( $\downarrow$ ) electrons. Second, the double occupancy probabilities on the sublattices are indicated by  $d_A$  and  $d_B$ , respectively. Third, the average hopping amplitude for the first and the next nearest neighbors (1st and 2nd n.n.) are defined by

$$\chi_{ij\sigma} \equiv \langle \hat{c}_{i\sigma}^\dagger \hat{c}_{j\sigma} \rangle_0 \equiv \begin{cases} \chi_{\sigma} & \text{for 1st n.n.,} \\ \chi_{S,\sigma} + e^{i\mathbf{Q}\cdot\mathbf{R}_i} \chi_{T,\sigma} & \text{for 2nd n.n.,} \end{cases} \quad (6)$$

with  $\chi_{S,\sigma} \equiv \frac{1}{2}(\chi_{AA\sigma} + \chi_{BB\sigma})$ ,  $\chi_{T,\sigma} \equiv \frac{1}{2}(\chi_{AA\sigma} - \chi_{BB\sigma})$ , where  $\chi_{AA\sigma}$  and  $\chi_{BB\sigma}$  denote respectively hopping of electron with the spin  $\sigma$  within sublattice A and B, and  $\chi_{AB\sigma} \equiv \chi_{\sigma}$  is the hopping between the sublattices (cf. Fig. 2 a). Fourth, the electron pairing amplitude between nearest neighbors, with spin-singlet and triplet components  $\Delta_S$  and  $\Delta_T$  are defined by

$$\Delta_{ij\sigma} \equiv \langle \hat{c}_{i\sigma} \hat{c}_{j\bar{\sigma}} \rangle_0 = -\tau_{ij} (\sigma \Delta_S + e^{i\mathbf{Q}\cdot\mathbf{R}_i} \Delta_T), \quad (7)$$

where  $\tau_{ij} \equiv 1$  for  $j = i \pm \hat{x}$ , and  $\tau_{ij} \equiv -1$  for  $j = i \pm \hat{y}$  to ensure the  $d$ -wave symmetry of  $\Delta_{ij\sigma}$ , and with  $\Delta_S \equiv \frac{1}{4}(\Delta_A + \Delta_B + \text{H.c.})$  and  $\Delta_T \equiv \frac{1}{4}(\Delta_A - \Delta_B + \text{H.c.})$  (cf. Fig. 2 b).

The mean field parameter defined above is determined numerically by minimizing the system's ground-state energy. However, in order to be sure that the self-consistent conditions are also fulfilled in a variational sense, we introduce additional constraints with the help of the the Lagrange multiplier method (cf. [32, 33]). Such an approach leads to the effective Hamiltonian of the following

form

$$\begin{aligned}\hat{K} = & W(n, m, \dots) - \sum_{\langle i,j \rangle, \sigma} (\lambda_{ij\sigma}^x (\hat{c}_{i\sigma}^\dagger \hat{c}_{j\sigma} - \chi_{ij\sigma}) + \text{H.c.}) \\ & - \sum_{\langle\langle i,j \rangle\rangle, \sigma} (\lambda_{ij\sigma}^x (\hat{c}_{i\sigma}^\dagger \hat{c}_{j\sigma} - \chi_{ij\sigma}) + \text{H.c.}) \\ & - \sum_{\langle i,j \rangle} (\lambda_{ij\sigma}^\Delta (\hat{c}_{i\sigma} \hat{c}_{j\bar{\sigma}} - \Delta_{ij\sigma}) + \text{H.c.}) \\ & - \sum_{i\sigma} (\lambda_{i\sigma}^n (\hat{n}_{i\sigma} - n_{i\sigma})) - \mu \sum_{i\sigma} \hat{n}_{i\sigma}. \quad (8)\end{aligned}$$

Next we derive the generalized grand potential function at temperature  $T > 0$ ,

$$\mathcal{F} = -\frac{1}{\beta} \ln \mathcal{Z}, \quad \text{with } \mathcal{Z} = \text{Tr} \left( e^{-\beta \hat{K}} \right), \quad (9)$$

with the Landau free energy equal to

$$F = \mathcal{F}_0 + \mu \Lambda n, \quad (10)$$

where  $\mathcal{F}_0$  denotes the value of  $\mathcal{F}$  obtained at the minimum, i.e. when the following conditions are fulfilled,

$$\frac{\partial \mathcal{F}}{\partial A_i} = 0, \quad \frac{\partial \mathcal{F}}{\partial \lambda_i} = 0, \quad \frac{\partial \mathcal{F}}{\partial d_A} = 0, \quad \frac{\partial \mathcal{F}}{\partial d_B} = 0, \quad (11)$$

where  $\{A_i\}$  denote the mean-field averages while  $\{\lambda_i\}$  refers to the Lagrange multipliers. The set of equations (11) can be subsequently solved using numerical methods. The results are presented in the Section IV.

### B. Extension: DE-GWF Approach

The SGA method described in the previous Section should be considered as a more sophisticated form of the Renormalized Mean Field Theory (RMFT), with the statistical consistency conditions included explicitly. In this Section we describe the Diagrammatic Expansion of the Gutzwiller Wave Function (DE-GWF) [34, 47–50]. With this method we extend our approach beyond RMFT in a systematic manner by including the nonlocal correlations in higher orders and thus reaching asymptotically the full Gutzwiller-wave-function solution step by step. It is important to note that within the extended approach the SGA is equivalent to the zeroth order form of the DE-GWF method. As the full approach is significantly more complicated than the SGA method, here we address the question of the full solution only for a pure superconducting phase. The determination of the full phase diagram, i.e., with the coexistent AF and CDW phases, is cumbersome within DE-GWF and must be discussed separately.

Similarly as before, in DE-GWF method, we are looking for the ground state of the system in the form given by Eq. (2). The general form of the  $\hat{P}$  operator takes the form [47–50]

$$\hat{P} \equiv \prod_i \hat{P}_i = \prod_i \sum_{\Gamma} \lambda_{i,\Gamma} |\Gamma\rangle \langle \Gamma|. \quad (12)$$

The variational parameters  $\lambda_{i,\Gamma} \in \{\lambda_{i\emptyset}, \lambda_{i\uparrow}, \lambda_{i\downarrow}, \lambda_{i\uparrow\downarrow}\}$  correspond to the four states of the local basis:  $|\emptyset\rangle_i$ ,  $|\uparrow\rangle_i$ ,  $|\downarrow\rangle_i$ , and  $|\uparrow\downarrow\rangle_i$ , respectively. In our analysis we assume the spatial homogeneity of the ourselves solutions, so  $\lambda_{i,\Gamma} \equiv \lambda_\Gamma$ . Moreover, we also limit to the spin-isotropic case, which means that  $\lambda_\uparrow = \lambda_\downarrow = \lambda$ . It has been shown by Bünemann et al. [47], that it is convenient to choose the  $\hat{P}_i$  operator so that it fulfills the following relation,

$$\hat{P}_i^2 = 1 + x \hat{d}_i^{\text{HF}}, \quad (13)$$

where  $x$  is yet another variational parameter and  $\hat{d}_i^{\text{HF}} = \hat{n}_{i\uparrow}^{\text{HF}} \hat{n}_{i\downarrow}^{\text{HF}}$ , where  $\hat{n}_{i\sigma}^{\text{HF}} = \hat{n}_{i\sigma} - n_0$  with  $n_0 = \langle \Psi_0 | \hat{n}_{i\sigma} | \Psi_0 \rangle$ . Eq. (13), together with the definition (12), allows us to express the variational parameters  $\lambda_\Gamma$  in terms of  $x$  (cf. Appendix A). In this manner, we are left only with a single variational parameter,  $x$ , over which we minimize the ground-state energy of the form from Eq. (3).

Using the condition (13), we can write all the relevant expectation values, which appear during the evaluation of Eq. (3), in the form of a power series with respect to the parameter  $x$ . As an example, we show here the power series for the hopping probability and the intersite Coulomb interaction terms (all other terms remaining in the Hamiltonian can be expressed in analogical form, cf. Ref. 49), are

$$\begin{cases} \langle \Psi | \hat{c}_{i\sigma}^\dagger \hat{c}_{j\sigma} | \Psi \rangle &= \sum_{k=0}^{\infty} \frac{x^k}{k!} \sum'_{l_1 \dots l_k} \langle \hat{c}_{i\sigma}^\dagger \hat{c}_{j\sigma} \hat{d}_{l_1 \dots l_k}^{\text{HF}} \rangle_0, \\ \langle \Psi | \hat{n}_{i\sigma} \hat{n}_{j\sigma'} | \Psi \rangle &= \sum_{k=0}^{\infty} \frac{x^k}{k!} \sum'_{l_1 \dots l_k} \langle \hat{n}_{i\sigma}^\dagger \hat{n}_{j\sigma'} \hat{d}_{l_1 \dots l_k}^{\text{HF}} \rangle_0, \end{cases} \quad (14)$$

where  $\hat{d}_{l_1 \dots l_k}^{\text{HF}} \equiv \hat{d}_{l_1}^{\text{HF}} \dots \hat{d}_{l_k}^{\text{HF}}$  with  $\hat{d}_{\emptyset}^{\text{HF}} \equiv 1$ , and the primed sums have the restrictions  $l_p \neq l_{p'}$  and  $l_p \neq i, j$ . Also, the following notation has been used  $\hat{c}_{i\sigma}^{(\dagger)} = \hat{P}_i \hat{c}_{i\sigma}^{(\dagger)} \hat{P}_i$  and  $\hat{n}_{i\sigma} = \hat{P}_i \hat{n}_{i\sigma} \hat{P}_i$ . By including the first 4-6 terms of the power series we are able to calculate with a desired accuracy the expectation value of the system energy. As one can see, the inclusion of higher order terms (i.e., those with  $k > 0$ ) leads to the situation in which the simple expression such as, e.g.,

$$\langle \Psi | \hat{c}_{i\sigma}^\dagger \hat{c}_{j\sigma} | \Psi \rangle = q_t \langle \Psi_0 | \hat{c}_{i\sigma}^\dagger \hat{c}_{j\sigma} | \Psi_0 \rangle, \quad (15)$$

are no longer valid due to the inclusion of nonlocal correlations of the increased range (caused by the appearance of the  $\hat{d}_{l_1 \dots l_k}^{\text{HF}}$  terms inside the expectation values  $\langle \dots \rangle_0$ ).

By using the Wick's theorem for the averages in the non-correlated state appearing in (14), one can express the average value of the systems energy in terms of the paramagnetic and superconducting lines, i.e., the correlation function that connect particular lattice sites, i.e.,

$$P_{ij} \equiv \langle \hat{c}_{i\sigma}^\dagger \hat{c}_{j\sigma} \rangle_0, \quad S_{ij} \equiv \langle \hat{c}_{i\uparrow}^\dagger \hat{c}_{j\downarrow}^\dagger \rangle_0. \quad (16)$$

Such a procedure leads in a natural manner to the diagrammatic representation of the energy expectation

value, in which the lattice sites play the role of the vertices for the diagrams and the paramagnetic or the superconducting lines are interpreted as their edges.

The minimization condition of the ground state energy (3) can be evaluated by introducing the effective single-particle Hamiltonian of the form

$$\hat{\mathcal{H}}_{\text{eff}} = \sum_{ij\sigma} t_{ij}^{\text{eff}} \hat{c}_{i\sigma}^\dagger \hat{c}_{j\sigma} + \sum_{ij} (\Delta_{ij}^{\text{eff}} \hat{c}_{i\uparrow}^\dagger \hat{c}_{j\downarrow}^\dagger + H.c.), \quad (17)$$

where the effective parameters appearing in this Hamiltonian are defined as

$$t_{ij}^{\text{eff}} \equiv \frac{\partial \mathcal{F}}{\partial P_{ij}}, \quad \Delta_{ij}^{\text{eff}} \equiv \frac{\partial \mathcal{F}}{\partial S_{ij}}. \quad (18)$$

By using the concept of the effective Hamiltonian one can derive the self-consistent equations for  $P_{ij}$  and  $S_{ij}$ , which can be then solved numerically. Such a procedure has to be supplemented with the concomitant energy minimization with respect to the variational parameter  $x$ . After determination of the value of  $x$ , together with those of the paramagnetic and superconducting lines, one can evaluate the so-called correlated superconducting gap defined as  $\Delta_{G|ij} \equiv \langle \Psi_G | \hat{c}_{i\uparrow}^\dagger \hat{c}_{j\downarrow}^\dagger | \Psi_G \rangle / \langle \Psi_G | \Psi_G \rangle$ , which represents the corresponding order parameter.

It should be noted that during the calculations one may limit to the terms with lines that correspond to distances smaller than  $R_{\text{max}}$ , as  $P_{ij}$  and  $S_{ij}$  with increasing distance  $|\Delta \mathbf{R}_{ij}| = |\mathbf{R}_i - \mathbf{R}_j|$  lead to systematically smaller contributions [50]. In our calculations we have taken  $\Delta R_{\text{max}}^2 = 10$ , which for the case of square lattice in a spatially homogeneous state and for the  $d$ -wave pairing symmetry, leads to 5 different superconducting lines. Each of those lines has its correspondent in the correlated state. The following notation is used in the subsequent discussion

$$\left\{ \begin{array}{l} \Delta_G^{(10)} \equiv \Delta_{G|ij}, \text{ for } \Delta \mathbf{R}_{ij} = (1, 0)a, \\ \Delta_G^{(20)} \equiv \Delta_{G|ij}, \text{ for } \Delta \mathbf{R}_{ij} = (2, 0)a, \\ \Delta_G^{(30)} \equiv \Delta_{G|ij}, \text{ for } \Delta \mathbf{R}_{ij} = (3, 0)a, \\ \Delta_G^{(21)} \equiv \Delta_{G|ij}, \text{ for } \Delta \mathbf{R}_{ij} = (2, 1)a, \\ \Delta_G^{(31)} \equiv \Delta_{G|ij}, \text{ for } \Delta \mathbf{R}_{ij} = (3, 1)a, \end{array} \right. \quad (19)$$

where  $a$  is the lattice constant.

## IV. RESULTS

### A. SC versus CDW stability in the Statistically Consistent Gutzwiller Approximation (SGA): commensurate phases

The numerical calculations were carried out for the two-dimensional, square lattice. Unless stated otherwise,

the following values of the microscopic parameters have been taken:  $t = -1$ ,  $J = |t|/3$ ,  $U = 20|t| \approx 2.5W$ , and  $\beta = 1500/|t|$ , where  $\beta \equiv 1/k_B T$  ( $T$  is the absolute temperature,  $k_B$  is the Boltzmann constant). We have checked out that for such choice of  $\beta$ , we reproduce the  $T = 0$  limit. To obtain results in physical units, all the energies should be multiplied by the physical value of  $|t|$  that is by 0.35 eV. The GSL library [51] has been used to solve the system up to 13 self-consistent equations. The typical accuracy of solution was  $10^{-10}$  for dimensionless quantities ( $\chi_\sigma$ ,  $\chi_{S,\sigma}$ ,  $\chi_{T,\sigma}$ ,  $\Delta_S$ ,  $\Delta_T$ , etc.)

In the panel composing Figure 3, we present the order parameters of the phases: AF, CDW, and SC, as well as the double occupancy,  $d$  (or  $d_A$  and  $d_B$  if it is necessary), all as a function of doping,  $\delta \equiv 1 - n$ . The order parameters for AF and CDW phases are the staggered magnetization  $m$  and the difference of the average number of electrons between the sublattices A and B,  $\delta_n$ , respectively. In case of SC, there are two order parameters (cf. [52, 53]), namely the singlet  $\Delta_S$  and the triplet  $\Delta_T$ . Note, that  $\Delta_T \neq 0$  only if  $m \neq 0$  and  $d$  splits to  $d_A \neq d_B$  only if  $\delta_n \neq 0$  (indices A and B refer to the different sublattices).

In Figure 3 *a*, we display the situation in the absence of the intersite Coulomb interaction term ( $V = 0$ ), whereas in panels *b* and *c*, the effect of the nonzero value of  $V$ , ranging from 0 to  $1.5|t|$ , on the SC gap component. One can see, that with the increasing value of  $V$  the SC order parameters are suppressed and in the underdoped region only a pure AF phase survives [54]. In Figure 3 *d*, the CDW order parameter ( $\delta_n$ ) is presented. For  $V < 1.85|t|$ , no stable CDW phase is observed, but when  $V$  reaches the critical value around  $1.85|t|$ , a region of a stable CDW order appears with  $\delta \approx 0.47$ . Upon increasing further the value of  $V$ , the CDW phase regime broadens up. Note, that here both AF and CDW states have the same modulation vector  $\mathbf{Q} = (\pi, \pi)$ .

The Figure 3 *e* shows the phase diagram for  $V/|t| = 2.5$ . For such relatively large values of  $V$  the SC order no longer appears and the CDW phase regime is broad. Note also, that the AF region is barely affected by the change of the  $V$  value in such a broad range.

We see that the regime of CDW stability with the vector  $\mathbf{Q}$ , commensurate with that of AF, order does not reflect properly the observed regime of coexistence depicted in Fig. 1. This question requires a more subtle analysis, as we discuss next. It is not strange that the CDW state is robust around  $\delta = n = 0.5$  point, as then every second site has a surcharge and thus the intersite interaction is diminished for  $\delta_n \approx n$ , which is the case of large  $V$ . A smaller values of  $V \lesssim |t|$  acts positively in the sense that it both reduces the upper concentration of the superconductivity disappearance (from  $\delta = 0.45$  to 0.3, as required for HTS), as well as makes the SC phase disappear for  $\delta < 0.1$ , where AF phase becomes the only stable state. On the other hand, CDW state is not yet

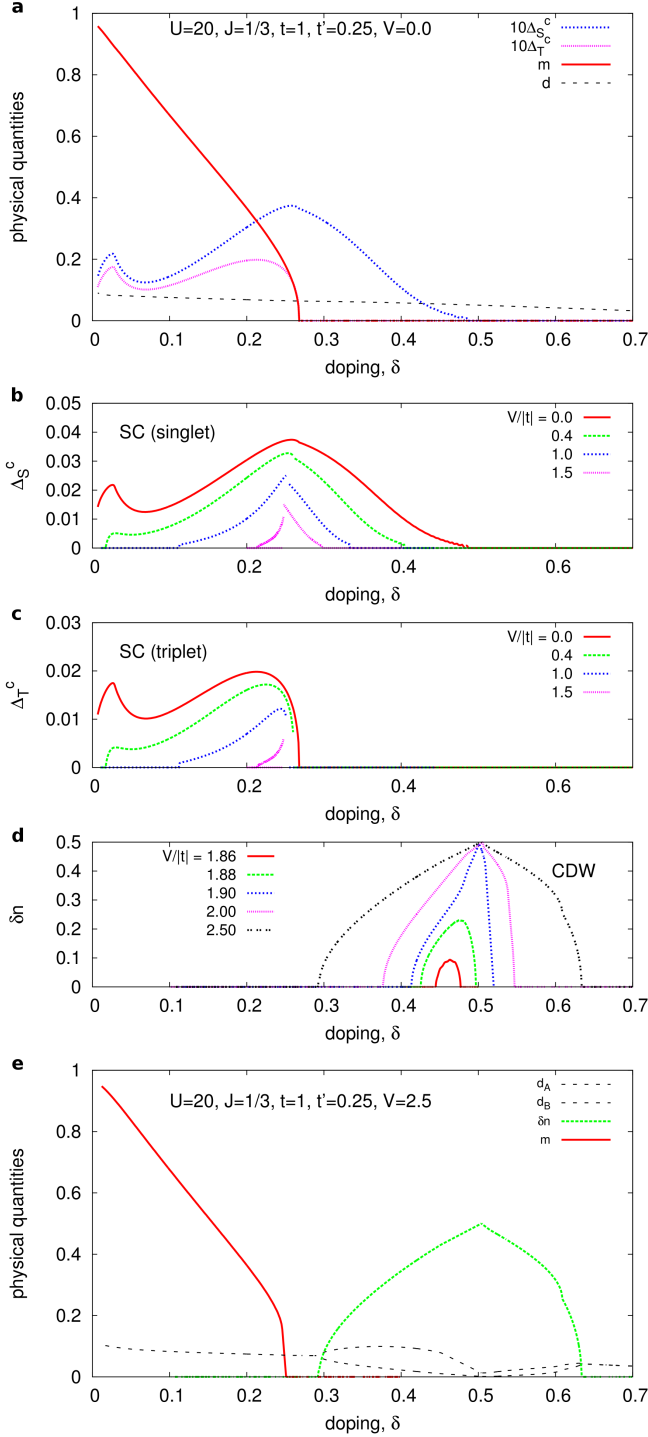


Figure 3. (Color online) Phase diagrams as a function of doping  $\delta$  for different values of parameters, as specified. *a*) AF and SC phases as well as the portion of the double occupied sites  $d^2 \approx 10^{-2}$  for  $V = 0$  (note, that on the plot  $d$  instead of  $d^2$  is shown). *b*) and *c*) superconducting order-parameter component  $\Delta_S^c$  and  $\Delta_T^c$ , respectively, for selected values of  $V/|t|$ . *d*) CDW order parameter as a function of  $V/|t|$ . *e*) the phase diagram for  $V/|t| = 2.5$ . Note that there is no stable SC phase for such a large value of  $V$ .

stable then. Hence, we have to discuss the CDW state onset for a realistic value of  $\mathbf{Q}$  taken from experiment (cf. next Section).

## B. Extension: SC and CDW stability

### 1. SC stability beyond SGA

In this subsection we discuss first the robustness of the pure superconducting phase within the DE-GWF method, i.e., when going beyond SGA (of RMFT type) within the extended  $t$ - $J$ - $U$ - $V$  model. First, we show the differences between the SGA and the DE-GWF for the selected set of the model parameters. The SC gap parameters obtained in the diagrammatic approach are displayed in Fig. 4 *a*. As one can see, the nearest neighboring pairing amplitude  $\Delta_G^{(10)}$  is by far the dominant one. Nonetheless, the remaining larger-distance contributions, may also become significant. Note, that in some doping regions different contributions can change the sign. For example, in the underdoped regime both  $\Delta_G^{(10)}$  and  $\Delta_G^{(30)}$  obey exactly the  $d$ -wave symmetry, but with the opposite phases. The situation is different within the SGA method, where the only nonzero pairing contribution taken into account is the nearest neighboring one. In Fig. 4 *b* we present the evolution of the  $\Delta_G^{(10)}$  gap with increasing order of calculations. The lowest dotted-dashed line corresponds to the SGA method which is also equivalent to the zeroth order of the DE-GWF approach. The differences between the green dotted line (the fourth order) and the black solid line (the fifth order) are very small which means that we have achieved a convergence with the assumed accuracy. As one can see, the two methods, SGA and DE-GWF, are qualitatively similar, but the correlations increase the pairing amplitude by 30%–40% as it encompasses also the more distant pairing amplitudes.

In Figure 5 we illustrate the influence of the intersite Coulomb repulsion on the stability of the paired phase within the DE-GWF method. As one can see, the upper critical doping for the disappearance of the superconducting phase in DE-GWF approach decreases again significantly when the  $V$  term is included, as it is in the SGA. One of the differences between the two considered methods is that inclusion of the higher order contributions leads to the modification of the so-called *non-BCS region* which is manifested by the kinetic energy gain at the transition to the SC phase. The kinetic energy gain is defined by

$$\Delta E_{\text{kin}} \equiv E_G^{SC} - E_G^{PM}, \quad E_G \equiv \frac{1}{N} \sum_{ij\sigma} t_{ij} \langle \hat{c}_{i\sigma}^\dagger \hat{c}_{j\sigma} \rangle_G, \quad (20)$$

where  $E_G^{SC}$  and  $E_G^{PM}$  correspond to the kinetic energies in SC and normal (paramagnetic, PM) phases, respectively. In the *BCS-like region*  $\Delta E_{\text{kin}} > 0$ , which is also



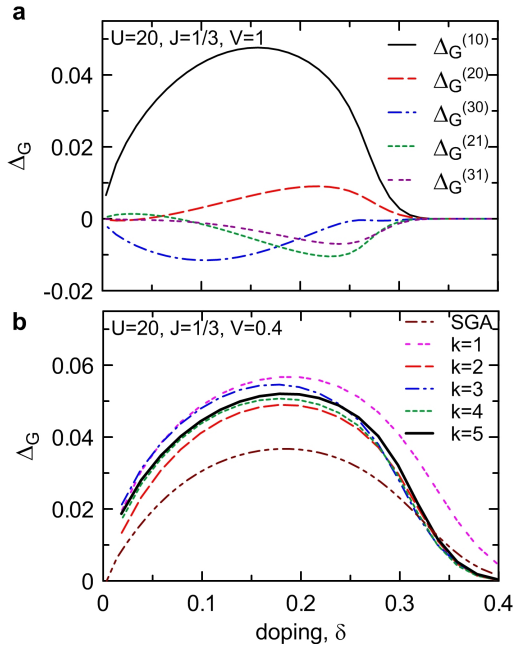


Figure 4. (Color online) *a*) Magnitudes of correlated gaps  $\Delta_G^{(mn)}$  (cf. Eq. (19)) between different neighbors as a function of doping for a selected set of microscopic parameters. *b*) Evolution of the nearest-neighbor correlated gap  $\Delta_G^{10}$  with the increasing order  $k$  of computations. The zeroth-order (SGA) results (the lowest line) are equivalent to the zeroth order DE-GWF approach. Note, that the lower critical concentration of the SC order is shown here to be 0 even for  $V > 0$ . It result from not including AF order in this graph. For  $V > 0$  the AF order competes with the SC in the underdoped regions and a pure AF phase wins over, as shown in Fig. 3, but if the AF order is not considered, the SC solution can survive, as it is shown here.

true for the BCS theory of the phonon-mediated superconductivity, whereas  $\Delta E_{\text{kin}} < 0$  for the non-BCS region. It should be noted that the non-BCS behavior has been detected experimentally [55, 56] for the underdoped samples, and shows the necessity of both including the higher orders to describe some important aspects of cuprate physics and using the extended model in a quantitative manner. We show here also that the intersite Coulomb repulsion promotes the non-BCS behavior by pushing it to higher doping values (cf. Fig. 5). Therefore, even though the intersite Coulomb interaction has a destructive effect by diminishing the condensation energy (cf. Fig. 5 *b*), it extends the region of the non-BCS state at the same time. In Figures 5 *b* and *c* we plot explicitly the contributions to the condensation energy that originates from either the intersite Coulomb repulsion term ( $V$ ) or the exchange interaction term ( $J$ ), respectively. The Coulomb repulsion term increases the energy of SC phase with respect to the normal (PM) state which means that it has a negative influence on the pairing strength. The opposite is true for

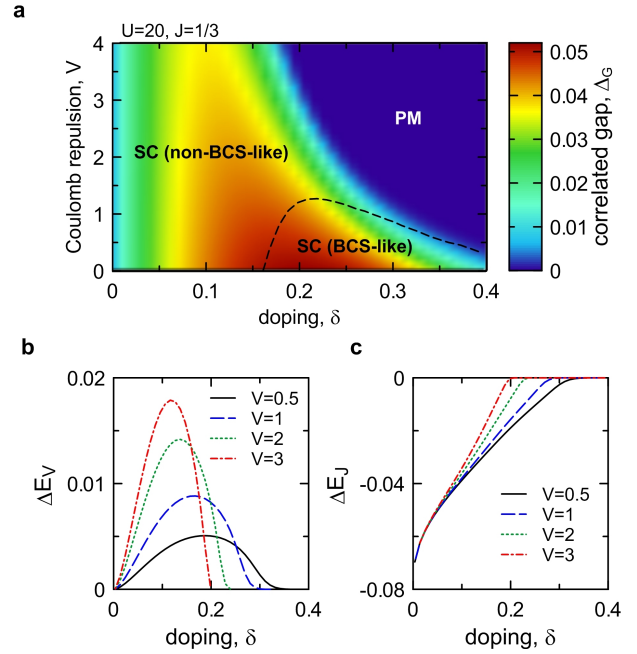


Figure 5. (Color online) *a*) Correlated gap value as a function of both doping ( $\delta$ ) and the intersite Coulomb repulsion ( $V$ ). One can distinguish between the two superconducting regimes: BCS-like and non-BCS, defined in main text. *b*) and *c*) Contribution to the condensation energy coming from the intersite Coulomb term  $\sim V$  and the exchange term  $\sim J$ , respectively. While the Coulomb repulsion  $\sim V$  increases the energy of SC with respect to the normal (PM) state, the opposite is true for the exchange part. In this sense, the Coulomb interactions  $\sim V$  play a destructive role for the pairing, whereas those  $\sim J$  provide the main role in it, together with the kinetic-energy gain in the underdoped regime.

the effect of the exchange term.

## 2. CDW vs. AF stability: incommensurate phase

Finally, we discuss the effect of choice of the CDW ordering type. Namely, so far we have assumed the simplest form of the modulation vector  $\mathbf{Q} = (\pi, \pi)$ , whereas in experiments, the CDW modulation vector is closer to  $\mathbf{Q}_{CDW} = (\frac{2}{3}\pi, 0)$  [9, 12]. Such a more realistic situation has been considered here as well, without including the SC phase so far, as the calculation of all the considered phases is quite cumbersome and should be discussed separately. From results depicted in Fig. 6 we see, that in this altered scenario the maximum of the CDW order parameter is shifted towards smaller dopings with respect to that of the previous situation. This is an important result, since it is observed that the CDW appears in the underdoped regime, close to the boundary of AF phase (cf. Fig. 1 and Ref. [9, 10]). This in turn suggests, that the full description including all phases (and their pos-

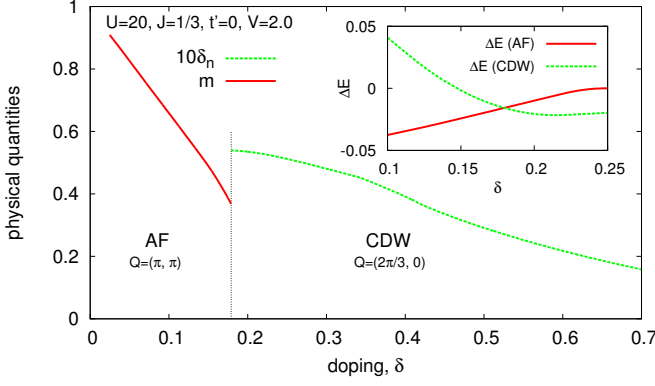


Figure 6. (Color online) Phase diagram with the inclusion of the AF and CDW orders. AF modulation vector is  $\mathbf{Q}_{AF} = (\pi, \pi)$  while the one corresponding to the CDW is  $\mathbf{Q}_{CDW} = (\frac{2}{3}\pi, 0)$ . Such form of CDW symmetry is close to the observed in the experiment. Neither SC order or hopping between the second neighboring sites ( $t' = 0$ ) was included here. In the inset, a difference between the energy of the two considered solutions and the plain paramagnetic one is presented. Note, that the energy of AF and CDW solution intersect, indicating the appearance of the first order transition.

sible coexistence), with such choice of the CDW modulation vector might bring the theory closer to experiment. Therefore, this result can be regarded as a starting point towards further quantitative investigations, including also the stability of the SC and AF states. Such a study may constitute a firm test for the one-band model of HTS.

## V. DISCUSSION

We have analyzed stability of AF, SC, CDW (and some of the possible coexistent phases) within the  $t$ - $J$ - $U$ - $V$  model. For this purpose we have used both the SGA and the DE-GWF methods. By using the former approach we have shown that CDW phase with  $\mathbf{Q} = (\pi, \pi)$  is stable only above a critical value of  $V$  (the intersite Coulomb repulsion), which is detrimental to SC phase stability. With the increasing  $V$ , the CDW stability range broadens up, whereas the SC phase is gradually suppressed. It is consistent with the experimental findings, according to which CDW and SC compete with each other. However, it should be mentioned that according to our calculations the CDW phase becomes stable in the overdoped regime, while in the experiment this phase is observed for smaller doping values. For  $\mathbf{Q} = (\frac{2}{3}\pi, 0)$ , the region of stability of CDW is wide, even for moderately small values of  $V$ . An interesting question is whether such a situation would change if we include in Fig. 6 the SC phase and/or go beyond the mean-field approach.

In the second part of the article, we have analyzed

first the influence of the higher order terms on the pure SC phase withing the DE-GWF method, including the fact that  $V > 0$ . One of the differences between the DE-GWF and SGA is that in the former approach the larger distance contributions to the pairing in real space appear (cf. Fig. 4), whereas in SGA only the nearest neighbor SC gap is present. The second result is that the magnitude of the SC order parameter in DE-GWF is enhanced by up to 40% as compared to the zero order calculations (SGA). In experiment, it is observed that CDW and SC phases can coexist [3, 6–11]. However, in SGA the increase of the  $V$  parameter suppresses SC before CDW appears. Therefore, the inclusion of the higher order terms that can lead to stability of the coexistent SC-CDW phase appears to be necessary. Finally, regarding the DE-GWF approach, the correlation effects taken into account through higher-order terms allow us to reproduce in a quantitative manner the appearance of the non-BCS behavior in the underdoped regime seen in the experiment [27, 57–60].

## Acknowledgments

We acknowledge the financial support through the Grant MAESTRO, No. DEC-2012/04/A/ST3/00342 from the National Science Centre (NCN) of Poland.

## Appendix A: Form of the $W$ function and mean-field renormalization factors

Using SGA, we need to calculate the expectation value of the Hamiltonian  $\langle \psi | \hat{\mathcal{H}}_{t-J-U-V} | \psi \rangle$  (cf. Eq. 3), namely

$$\begin{aligned}
 W = \langle \hat{\mathcal{H}}_{t-J-U-V} \rangle = & t \sum_{\langle i,j \rangle, \sigma} ((\hat{c}_{i\sigma}^\dagger \hat{c}_{j\sigma}) + H.c.) \\
 & + t' \sum_{\langle\langle i,j \rangle\rangle, \sigma} ((\hat{c}_{i\sigma}^\dagger \hat{c}_{j\sigma}) + H.c.) + J \sum_{\langle i,j \rangle} \langle \hat{\mathbf{S}}_i \cdot \hat{\mathbf{S}}_j \rangle \\
 & + U \sum_i \langle \hat{n}_{i\uparrow} \hat{n}_{i\downarrow} \rangle + \underbrace{\left( \tilde{V} - \frac{1}{4} J \right)}_V \sum_{\langle i,j \rangle, \sigma, \sigma'} \langle \hat{n}_{i\sigma} \hat{n}_{j\sigma'} \rangle, \quad (A1)
 \end{aligned}$$

where for simplicity we denote  $\langle \Psi | \dots | \Psi \rangle \equiv \langle \dots \rangle$ . However, this is a non-trivial task, since the wave function  $|\Psi\rangle$  is unknown. The standard Gutzwiller procedure in such cases [45, 46] is to assume, that  $|\Psi\rangle = \hat{P} |\Psi_0\rangle$ , where  $|\Psi_0\rangle$  is a simple, non-correlated wave function, and  $\hat{P} = \prod_i \hat{P}_i$  is the operator, which changes the likelihood of sites to be occupied by certain states. In general form,

$$\begin{aligned}
 \hat{P}_i = & \sum_j \lambda_{ij} |\Gamma_j\rangle_{ii} \langle \Gamma_j| = \lambda_{i,0} (1 - \hat{n}_{i\uparrow})(1 - \hat{n}_{i\downarrow}) + \\
 & \lambda_{i,\uparrow} \hat{n}_{i\uparrow} (1 - \hat{n}_{i\downarrow}) + \lambda_{i,\downarrow} (1 - \hat{n}_{i\uparrow}) \hat{n}_{i\downarrow} + \lambda_{i,d} \hat{n}_{i\uparrow} \hat{n}_{i\downarrow}. \quad (A2)
 \end{aligned}$$

Following Ref. [47], we assume that  $\hat{P}_i^2 \equiv 1 + x_i \hat{n}_{i\uparrow}^{HF} \hat{n}_{i\downarrow}^{HF}$ , with  $\hat{n}_{i\sigma}^{HF} \equiv \hat{n}_{i\sigma} - n_{i\sigma}$ . Next,  $\hat{P}_i^2$  acting on the local basis,



$|\emptyset\rangle_i, |\uparrow\rangle_i, |\downarrow\rangle_i, |\uparrow\downarrow\rangle_i$ , one can yields:

$$\begin{cases} \lambda_{i,0}^2 &= 1 + x_i n_{i\sigma} n_{i\bar{\sigma}}, \\ \lambda_{i,\sigma}^2 &= 1 - x_i (1 - n_{i\sigma}) n_{i\bar{\sigma}}, \\ \lambda_{i,d}^2 &= 1 + x_i (1 - n_{i\sigma})(1 - n_{i\bar{\sigma}}), \end{cases} \quad (\text{A3})$$

where  $x_i$  is a variational parameter. When  $\forall_i x_i = 0$ , then the operator  $\hat{P} = \mathbb{1}$  and  $|\Psi\rangle = |\Psi_0\rangle$ , but when  $\exists_i x_i < 0$ , then the likelihood that site  $i$  has two electrons is reduced. Since the the average number of electrons in the system should remain constant,  $x_i < 0$  requires, that the number of the single occupied sites is increased and the number of empty sites is reduced at the same times.

The meaning of parameter  $x_i$  is not easy to provide. Therefore we introduce  $d_i^2$  as the double-occupancy probability at site  $i$ , namely,

$$\langle \Psi | \hat{n}_{i\uparrow} \hat{n}_{i\downarrow} | \Psi \rangle \equiv d_i^2. \quad (\text{A4})$$

We can relate  $d_i^2$  to the  $x_i$  parameter, since

$$d_i^2 = \langle \Psi | \hat{n}_{i\uparrow} \hat{n}_{i\downarrow} | \Psi \rangle = \langle \Psi_0 | \hat{P}_i \hat{n}_{i\uparrow} \hat{n}_{i\downarrow} \hat{P}_i | \Psi_0 \rangle = \lambda_{i,d}^2 n_{i\uparrow} n_{i\downarrow}, \quad (\text{A5})$$

where we have assumed that  $\langle \Psi_0 | \hat{n}_{i\uparrow} \hat{n}_{i\downarrow} | \Psi_0 \rangle \equiv \langle \hat{n}_{i\uparrow} \hat{n}_{i\downarrow} \rangle_0 = n_{i\uparrow} n_{i\downarrow}$ , i.e., that the following averages  $\langle \hat{c}_{i\uparrow}^\dagger \hat{c}_{i\downarrow} \rangle_0$  and  $\langle \hat{c}_{i\uparrow}^\dagger \hat{c}_{i\downarrow} \rangle_0$  are zero. Using Eqs. (A3)–(A5), we can show, that

$$x_i \equiv \frac{d^2 - n_{i\uparrow} n_{i\downarrow}}{n_{i\uparrow} n_{i\downarrow} (1 - n_{i\uparrow})(1 - n_{i\downarrow})}, \quad (\text{A6})$$

and as a result, can rewrite the expressions (A3) in the form:

$$\lambda_{i,0}^2 = \frac{1 + d^2 - n_\sigma - n_{\bar{\sigma}}}{(1 - n_\sigma)(1 - n_{\bar{\sigma}})}, \quad (\text{A7})$$

$$\lambda_{i,\sigma}^2 = \frac{n_\sigma - d^2}{n_\sigma (1 - n_{\bar{\sigma}})}, \quad (\text{A8})$$

$$\lambda_{i,d}^2 = \frac{d^2}{n_\sigma n_{\bar{\sigma}}}. \quad (\text{A9})$$

To calculate the averages appearing in Eq. (A1), we need one more (partial) result, namely

$$\hat{P}_i \hat{c}_{i\sigma}^\dagger \hat{P}_i = (\lambda_\sigma \hat{n}_{i\sigma} (1 - \hat{n}_{i\bar{\sigma}}) + \lambda_d \hat{n}_{i\sigma} \hat{n}_{i\bar{\sigma}}) \hat{c}_{i\sigma}^\dagger (\lambda_{\bar{\sigma}} \hat{n}_{i\bar{\sigma}} (1 - \hat{n}_{i\sigma}) + \lambda_0 (1 - \hat{n}_{i\sigma})(1 - \hat{n}_{i\bar{\sigma}})) = (\alpha_{i\sigma} + \beta_{i\sigma} \hat{n}_{i\bar{\sigma}}^{HF}) \hat{c}_{i\sigma}^\dagger, \quad (\text{A10})$$

where

$$\alpha_{i\sigma} = \sqrt{\frac{(n_{i\sigma} - d_i^2)(1 - n + d_i^2)}{n_{i\sigma}(1 - n_{i\sigma})}} + |d_i| \sqrt{\frac{n_{i\bar{\sigma}} - d_i^2}{n_{i\sigma}(1 - n_{i\sigma})}}, \quad (\text{A11})$$

$$\beta_{i\sigma} = -\sqrt{\frac{(n_{i\sigma} - d_i^2)(1 - n + d_i^2)}{n_{i\sigma}(1 - n_{i\sigma})(1 - n_{i\bar{\sigma}})^2}} + |d_i| \sqrt{\frac{n_{i\bar{\sigma}} - d_i^2}{n_\sigma n_{\bar{\sigma}}^2 (1 - n_\sigma)}}. \quad (\text{A12})$$

Note that for  $\hat{P}_i \hat{c}_{i\sigma} \hat{P}_i$  we would obtain the same result as above. Using above expressions, one can calculate other average, e.g., the average of the hopping term is then

$$\begin{aligned} \langle \hat{c}_{i\sigma}^\dagger \hat{c}_{j\sigma} \rangle &= \langle \hat{P}_i \hat{P}_j \hat{c}_{i\sigma}^\dagger \hat{c}_{j\sigma} \hat{P}_i \hat{P}_j \rangle_0 = \langle \hat{P}_i \hat{c}_{i\sigma}^\dagger \hat{P}_i \hat{P}_j \hat{c}_{j\sigma} \hat{P}_j \rangle_0 \\ &= \alpha_{i\sigma} \alpha_{j\sigma} \langle \hat{c}_{i\sigma}^\dagger \hat{c}_{j\sigma} \rangle_0 + \alpha_{i\sigma} \beta_{j\sigma} \langle \hat{n}_{i\bar{\sigma}}^{HF} \hat{c}_{i\sigma}^\dagger \hat{c}_{j\sigma} \rangle_0 \\ &\quad + \alpha_{j\sigma} \beta_{i\sigma} \langle \hat{n}_{j\bar{\sigma}}^{HF} \hat{c}_{i\sigma}^\dagger \hat{c}_{j\sigma} \rangle_0 + \beta_{i\sigma} \beta_{j\sigma} \langle \hat{n}_{i\bar{\sigma}}^{HF} \hat{n}_{j\bar{\sigma}}^{HF} \hat{c}_{i\sigma}^\dagger \hat{c}_{j\sigma} \rangle_0. \end{aligned} \quad (\text{A13})$$

Using the Wick's theorem we can check that  $\langle \hat{n}_{i\bar{\sigma}}^{HF} \hat{c}_{i\sigma}^\dagger \hat{c}_{j\sigma} \rangle_0 = 0$  and  $\alpha_{j\sigma} \beta_{i\sigma} \langle \hat{n}_{j\bar{\sigma}}^{HF} \hat{c}_{i\sigma}^\dagger \hat{c}_{j\sigma} \rangle_0 = 0$ , as far as we assume that there is no onsite pairing of electrons,  $\langle \hat{c}_{i\sigma}^\dagger \hat{c}_{i\bar{\sigma}} \rangle_0 = 0$ , and hopping does not change spin,  $\langle \hat{c}_{i\sigma}^\dagger \hat{c}_{j\bar{\sigma}} \rangle_0 = 0$ . The last average in Eq. A13 is usually non-zero, but small, therefore it can be neglected here.

Hence, we are left with

$$\langle \hat{c}_{i\sigma}^\dagger \hat{c}_{j\sigma} \rangle \approx \alpha_{i\sigma} \alpha_{j\sigma} \langle \hat{c}_{i\sigma}^\dagger \hat{c}_{j\sigma} \rangle_0. \quad (\text{A14})$$

In the simplest case, where neither AF nor CDW ordering are present, we have  $\alpha_{i\sigma} = \alpha_{j\sigma} = \alpha$  and thus

$$\alpha^2 = g_t \equiv \frac{n - 2d^2}{n(1 - n/2)} \left( \sqrt{1 - n + d^2} + |d| \right)^2, \quad (\text{A15})$$

what is the Gutzwiller factor for the hopping part, well known from the literature, cf. Refs. [30, 61–63].

In a similar manner, the other averages appearing in Eq. (A1) can also be calculated. To provide one more example, we show explicitly here how to calculate the last term,  $\langle \hat{n}_{i\sigma} \hat{n}_{j\sigma} \rangle$ , requiring perhaps the most non-trivial calculations, and rarely discussed in the literature. To abbreviate the length of the expressions, we assume here for moment, that we are interested only in AF order. The generalization to the case of CDW order (or others) is not difficult and it can be left to the Reader. Note that assuming AF ordering requires that  $n_\sigma$  on A sublattice is equal to  $n_{\bar{\sigma}}$  on the B sublattice.

In such a case,

$$\begin{aligned}
\Lambda^{-1} \sum_{\langle i,j \rangle, \sigma, \sigma'} \langle \hat{n}_{i\sigma} \hat{n}_{j\sigma'} \rangle &= \Lambda^{-1} \sum_{\langle i,j \rangle, \sigma, \sigma'} \langle \hat{P}_i \hat{n}_{i\sigma} \hat{P}_i \hat{P}_j \hat{n}_{j\sigma'} \hat{P}_j \rangle_0 = \\
&= \Lambda^{-1} \sum_{\langle i,j \rangle, \sigma, \sigma'} \langle (\hat{n}_{i\sigma} + (\lambda_d^2 - \lambda_\sigma^2) \hat{n}_{i\sigma} \hat{n}_{i\bar{\sigma}}^{HF}) (\hat{n}_{j\sigma'} + (\lambda_d^2 - \lambda_{\sigma'}^2) \hat{n}_{j\sigma'} \hat{n}_{j\bar{\sigma}'}^{HF}) \rangle_0 \\
&\approx \Lambda^{-1} \sum_{\langle i,j \rangle, \sigma} \langle n_{i\sigma} n_{j\sigma} \rangle_0 + \langle n_{i\sigma} n_{j\bar{\sigma}} \rangle_0 \\
&\quad + \left( \langle \hat{n}_{j\bar{\sigma}} \rangle_0 \langle \hat{n}_{i\bar{\sigma}} \hat{n}_{j\sigma}^{HF} \rangle_0 + \langle \hat{n}_{j\bar{\sigma}} \rangle_0 \langle \hat{n}_{i\sigma} \hat{n}_{j\bar{\sigma}}^{HF} \rangle_0 + \langle \hat{n}_{i\sigma} \rangle_0 \langle \hat{n}_{j\sigma} \hat{n}_{i\bar{\sigma}}^{HF} \rangle_0 + \langle \hat{n}_{i\sigma} \rangle_0 \langle \hat{n}_{j\bar{\sigma}} \hat{n}_{i\bar{\sigma}}^{HF} \rangle_0 \right) (\lambda_d^2 - \lambda_\sigma^2) \\
&\quad + (\lambda_d^2 - \lambda_\sigma^2) (\lambda_d^2 - \lambda_{\sigma'}^2) \langle \hat{n}_{i\sigma} \rangle_0 \langle \hat{n}_{j\sigma} \rangle_0 \langle \hat{n}_{i\bar{\sigma}}^{HF} \hat{n}_{j\bar{\sigma}}^{HF} \rangle_0 + (\lambda_d^2 - \lambda_\sigma^2) (\lambda_d^2 - \lambda_{\sigma'}^2) \langle \hat{n}_{i\sigma} \rangle_0 \langle \hat{n}_{j\bar{\sigma}} \rangle_0 \langle \hat{n}_{i\bar{\sigma}}^{HF} \hat{n}_{j\bar{\sigma}}^{HF} \rangle_0 \\
&= 2n^2 + (-4\chi^2 + 4\Delta_S^2 + 4\Delta_T^2) (1 + n_\sigma (\lambda_d^2 - \lambda_\sigma^2) + n_{\bar{\sigma}} (\lambda_d^2 - \lambda_{\bar{\sigma}}^2)) \\
&\quad + 4n_\sigma (\lambda_d^2 - \lambda_\sigma^2) n_{\bar{\sigma}} (\lambda_d^2 - \lambda_{\bar{\sigma}}^2) (-\chi^2) + 2 \left( [n_\sigma (\lambda_d^2 - \lambda_\sigma^2)]^2 + [n_{\bar{\sigma}} (\lambda_d^2 - \lambda_{\bar{\sigma}}^2)]^2 \right) (\Delta_S^2 + \Delta_T^2) \\
&= 2n^2 + 4g_v^\chi (-\chi^2) + 4g_v^\Delta (\Delta_S^2 + \Delta_T^2),
\end{aligned} \tag{A16}$$

where

$$g_v^\chi \equiv (1 + n_\sigma (\lambda_d^2 - \lambda_\sigma^2) + n_{\bar{\sigma}} (\lambda_d^2 - \lambda_{\bar{\sigma}}^2) + n_\sigma (\lambda_d^2 - \lambda_\sigma^2) n_{\bar{\sigma}} (\lambda_d^2 - \lambda_{\bar{\sigma}}^2)), \tag{A17}$$

$$g_v^\Delta \equiv \left( 1 + n_\sigma (\lambda_d^2 - \lambda_\sigma^2) + n_{\bar{\sigma}} (\lambda_d^2 - \lambda_{\bar{\sigma}}^2) + \frac{1}{2} \left( [n_\sigma (\lambda_d^2 - \lambda_\sigma^2)]^2 + [n_{\bar{\sigma}} (\lambda_d^2 - \lambda_{\bar{\sigma}}^2)]^2 \right) \right). \tag{A18}$$

The “ $\approx$ ” sign in Eq. (A16) results from the fact, that we neglected terms proportional to  $\chi^4$ ,  $\Delta_S^4$ ,  $\Delta_T^4$  and  $n_\sigma n_{\bar{\sigma}} \chi^2$ . Note that if no AF order is considered ( $m = 0$ ), then  $n_\sigma = n_{\bar{\sigma}} = n/2$  and then

$$g_v^\chi = g_v^\Delta = \left( \frac{2d^2 + n(1-n)}{n(1-n/2)} \right)^2. \tag{A19}$$

## Appendix B: Two ways of defining the Gutzwiller factor in the presence of extra orderings

In this Appendix we show that introduction of extra orderings, such as AF or CDW, can lead to a specific ambiguity in determining the final form of the Gutzwiller renormalization factors. We explain also, how we have decided to select a particular form used in main text.

For simplicity, we assume here, that  $U \rightarrow \infty$ , resulting in  $d \rightarrow 0$ . Furthermore, to make our arguments easy to follow, we consider only the AF order and focus on the example of Gutzwiller factor for the hopping term that has been already discussed in the foregoing Appendix (cf. Eq. (A15)). The generalization to other states and to other averages is straightforward.

In the preceding Appendix one of our objective was to find an operator  $\hat{P}$  that leads to the following approximation

$$\langle \Psi | \hat{c}_{i\sigma}^\dagger \hat{c}_{j\sigma} | \Psi \rangle \approx \langle \Psi_0 | \hat{P}_i \hat{c}_{i\sigma}^\dagger \hat{P}_i \hat{P}_j \hat{c}_{j\sigma} \hat{P}_j | \Psi_0 \rangle \tag{B1}$$

The question is how to find such a function  $g_t(n_{i\sigma}, n_{i\bar{\sigma}}, d, \dots)$  (called the Gutzwiller renormalization

factor), that

$$\langle \Psi_0 | \hat{P}_i \hat{c}_{i\sigma}^\dagger \hat{P}_i \hat{P}_j \hat{c}_{j\sigma} \hat{P}_j | \Psi_0 \rangle = g_t \langle \Psi_0 | \hat{c}_{i\sigma}^\dagger \hat{c}_{j\sigma} | \Psi_0 \rangle. \tag{B2}$$

This renormalization factor can be obtained, by comparison of the likelihood of a specific process (in this example hopping) in the correlated  $|\Psi\rangle$ , and in the uncorrelated  $|\Psi_0\rangle$  states, namely

$$g_t(n_{i\sigma}, n_{i\bar{\sigma}}, d, \dots) \approx \frac{\langle \Psi | \hat{c}_{i\sigma}^\dagger \hat{c}_{j\sigma} | \Psi \rangle}{\langle \Psi_0 | \hat{c}_{i\sigma}^\dagger \hat{c}_{j\sigma} | \Psi_0 \rangle}. \tag{B3}$$

Let us assume that there are on average  $n$  electrons per site and the staggered magnetization is equal to  $m$ . In the non-correlated case ( $U = 0$ ), there is in average  $n_\sigma \equiv n_{A\sigma} = \frac{1}{2}(n + \sigma m)$  electrons with spin  $\sigma$  per site for the A sublattice and  $n_{\bar{\sigma}} \equiv n_{B\sigma} = \frac{1}{2}(n - \sigma m)$  for the B sublattice. Additionally, on average,  $n_{\uparrow\downarrow} = n_{A\uparrow} n_{A\downarrow} = n_{B\uparrow} n_{B\downarrow}$  and consequently,  $n_\emptyset = (1 - n_{A\uparrow})(1 - n_{A\downarrow}) = (1 - n_{B\uparrow})(1 - n_{B\downarrow})$  (cf. Table I).

In the correlated state  $|\Psi\rangle$  the double occupancy  $d^2$  should be smaller than for  $|\Psi_0\rangle$ . The appropriate adjustment is made by selecting a proper form of the  $\hat{P}$  operator (cf. Refs. [45, 46]). In the case of  $U \rightarrow \infty$ , there is  $\forall_i \lambda_{i,d} \equiv 0$  (cf. the general form of  $\hat{P}$ , Eq. (A2)). However, by changing the probability of states to be doubly occupied, we change also the average number of the electrons in the system. To avoid this, the weights  $\lambda_{i,0}$ ,  $\lambda_{i,\uparrow}$  and  $\lambda_{i,\downarrow}$  need to be modified as well.

There are two intuitive ways how this can be achieved, namely

1. We can “split” every double occupancy, separating the electrons (one  $\uparrow$  and one  $\downarrow$ ) to different, previ-

Table I. Likelihood of a site being in the certain state (uncorrelated case  $|\Psi_0\rangle$ ).

state	for A sublattice	for B sublattice
$ \uparrow\rangle$ or $ \uparrow\downarrow\rangle$	$n_{A\uparrow} = \frac{1}{2}(n+m)$	$n_{B\uparrow} = \frac{1}{2}(n-m)$
$ \downarrow\rangle$ or $ \uparrow\downarrow\rangle$	$n_{A\downarrow} = \frac{1}{2}(n-m)$	$n_{B\downarrow} = \frac{1}{2}(n+m)$
$ \uparrow\rangle$	$n_{A\uparrow}(1-n_{A\downarrow})$	$n_{B\uparrow}(1-n_{B\downarrow})$
$ \downarrow\rangle$	$n_{A\downarrow}(1-n_{A\uparrow})$	$n_{B\downarrow}(1-n_{B\uparrow})$
$ \emptyset\rangle$	$(1-n_{A\uparrow})(1-n_{A\downarrow})$	$(1-n_{B\uparrow})(1-n_{B\downarrow})$
$ \uparrow\downarrow\rangle$	$n_{A\uparrow}n_{A\downarrow}$	$n_{B\uparrow}n_{B\downarrow}$

Table II. Likelihood of a site being in the certain state (correlated case  $|\Psi\rangle$ ). In the table, only the results for the A sublattice were shown. For the B sublattice simply  $n_{B\sigma} = n_{A\bar{\sigma}}$ .

state	scheme 1. (“splitting”)	scheme 2. (“erasing”)
$ \uparrow\rangle$	$n_{A\uparrow} = \frac{1}{2}(n+m)$	$n_{A\uparrow}(1-n_{A\downarrow})\frac{n}{n-2n_{A\uparrow}n_{A\downarrow}}$
$ \downarrow\rangle$	$n_{A\downarrow} = \frac{1}{2}(n-m)$	$n_{A\downarrow}(1-n_{A\uparrow})\frac{n}{n-2n_{A\uparrow}n_{A\downarrow}}$
$ \emptyset\rangle$	$1-n_{A\uparrow}-n_{A\downarrow}$	$1-n_{A\uparrow}-n_{A\downarrow}$
$ \uparrow\downarrow\rangle$	0	0

ously empty sites. Such operation would not change the global magnetization of the system ( $m \equiv n_{\uparrow}-n_{\downarrow}$ ) but it would modify the proportion of the number of the single occupied  $|\uparrow\rangle$  states to the number of  $|\downarrow\rangle$  states.

2. We can “erase” the double occupancies. However, such action would change the number of electrons in the system. Therefore, to restore the previous number of electrons, we can *proportionally* add *up* and *down* electrons to previously empty sites. This operation would keep the proportion of the number of single occupied states with the spin *up* to those with the spin *down*, but it would modify the global magnetization of the system.

Each of the presented schemes, leads to a different probability of sites to be in certain states, as it is displayed in the Table II. Note, that in the first scheme, the proportion of  $|\uparrow\rangle$  states is the same as “ $|\uparrow\rangle$  or  $|\uparrow\downarrow\rangle$ ” states in the Table I. In the second scheme, after erasing the doubly occupied states, the number of the electrons has changed from  $n$  to  $n-n_{A\sigma}n_{A\bar{\sigma}}$  in the A sublattice and to  $n-n_{B\sigma}n_{B\bar{\sigma}}$  in the B sublattice. Therefore, to restore the previous number of electrons in the system, the probability that the state will have single electron  $\sigma$  was renormalized by the factor  $n/(n-2n_{A\uparrow}n_{A\downarrow}) \equiv n/(n-2n_{B\uparrow}n_{B\downarrow})$ .

Next, it is possible to derive the  $g_t$  Gutzwiller factor for the hopping term in both schemes. For the hopping to occur in the correlated state, there needs to be a site occupied by a single electron with the spin  $\sigma$ , while the neighboring site needs to be empty. Therefore, by com-

paring the amplitudes of the bra and the ket contributions of  $\langle\Psi|\hat{c}_{i\sigma}^\dagger\hat{c}_{j\sigma}|\Psi\rangle$ , and with the help of Table II, we can write that in the first scheme,

$$\langle\Psi|\hat{c}_{i\sigma}^\dagger\hat{c}_{j\sigma}|\Psi\rangle \stackrel{(1)}{=} \sqrt{n_{A\sigma}n_{B\sigma}}(1-n). \quad (B4)$$

whereas in the second scheme,

$$\langle\Psi|\hat{c}_{i\sigma}^\dagger\hat{c}_{j\sigma}|\Psi\rangle \stackrel{(2)}{=} \sqrt{\frac{n_{A\sigma}(1-n_{A\bar{\sigma}})n_{B\sigma}(1-n_{B\bar{\sigma}})}{(n-2n_{A\uparrow}n_{A\downarrow})(n-2n_{B\uparrow}n_{B\downarrow})}}n(1-n). \quad (B5)$$

Analogically, we can calculate the hopping probability in the uncorrelated state. Namely, the hopping can occur when either one site has electron with the spin  $\sigma$  or it is doubly occupied, and when either the neighboring site is empty or has one electron with the spin  $\bar{\sigma}$  (cf. also [64]). Using Table I, we obtain

$$\langle\Psi_0|\hat{c}_{i\sigma}^\dagger\hat{c}_{j\sigma}|\Psi_0\rangle = \sqrt{n_{A\sigma}(1-n_{B\sigma})n_{B\sigma}(1-n_{A\sigma})}. \quad (B6)$$

Using Eq. (B3), we obtain either

$$g_t^{(1)} = \frac{1-n}{\sqrt{(1-n_{\uparrow})(1-n_{\downarrow})}}, \quad (B7)$$

or

$$g_t^{(2)} = \frac{1-n}{1-\frac{2n_{\uparrow}n_{\downarrow}}{n}}, \quad (B8)$$

respectively, where we denoted  $n_{\sigma} \equiv n_{A\sigma} = n_{B\bar{\sigma}}$ . Both  $g_t^{(1)}$  and  $g_t^{(2)}$  are present in the literature, for example  $g_t^{(2)}$  in Refs. [29, 30, 61, 63], whereas  $g_t^{(1)}$  is identical with the zero-order renormalization factors of the DE-GWF method Refs. [47–50, 65].

Note that if no AF order is present,

$$g_t^{(1)} \equiv g_t^{(2)} \equiv g_t = \frac{1-n}{1-n/2}, \quad (B9)$$

and there is no difference between  $g_t^{(1)}$  and  $g_t^{(2)}$  anymore (cf. also Eq. (A15) and take  $d=0$ ).

If instead, CDW (with no AF) order were considered, we would simply take in Eqs. (B4)–(B6)  $n_{A\sigma} = n_A$  and  $n_{B\sigma} = n_B$ , so that  $n_A \neq n_B$ . In such a case we have also  $g_t^{(1)} \neq g_t^{(2)}$ .

The above discussion, can be easily carried out for other Gutzwiller factors, that renormalize the averages other than the hopping. In effect, the results will become method dependent. Explicitly, it has also been checked that the two schemes lead to substantially different outputs, especially regarding the stability of the AF phase. In the first scheme (used in main text of this paper), AF phase is stable in the wide range of doping, from 0 to about  $\delta_{max} = 0.27$  (cf. Fig. 3). By using the second scheme instead, the AF phase is stable only very close to the half-filling with  $\delta_{max} < 0.006$  (cf. our previous paper [26]).

In this paper, we have decided to use the first scheme, since we wanted to compare our present SGA results to those obtained within the DE-GWF approach. And, as

it has been mentioned already, in the zeroth-order of the DE-GWF method, the renormalization factors are identical to those from the first scheme.

- 
- [1] E. J. W. Verwey, *Nature* **144**, 327 (1939).
  - [2] E. J. W. Verwey and P. W. Haayman, *Physica* **8**, 979 (1941).
  - [3] B. Keimer, S. A. Kivelson, M. R. Norman, S. Uchida, and J. Zaanen, *Nature* **518**, 179 (2015).
  - [4] J. M. Tranquada, B. J. Sternlieb, J. D. Axe, Y. Nakamura, and S. Uchida, *Nature* **375**, 561 (1995).
  - [5] J. P. Attfield, *Solid State Sciences* **8**, 861 (2006).
  - [6] G. Ghiringhelli, M. Le Tacon, M. Minola, S. Blanco-Canosa, C. Mazzoli, N. B. Brookes, G. M. De Luca, A. Frano, D. G. Hawthorn, F. He, T. Loew, M. M. Sala, D. C. Peets, M. Salluzzo, E. Schierle, R. Sutarto, G. A. Sawatzky, E. Weschke, B. Keimer, and L. Braicovich, *Science* **337**, 821 (2012).
  - [7] R. Comin, A. Frano, M. M. Yee, Y. Yoshida, H. Eisaki, E. Schierle, E. Weschke, R. Sutarto, F. He, A. Soumyanarayanan, Y. He, M. Le Tacon, I. S. Elfimov, J. E. Hoffman, G. A. Sawatzky, B. Keimer, and A. Damascelli, *Science* **343**, 390 (2014).
  - [8] E. H. da Silva Neto, P. Aynajian, A. Frano, R. Comin, E. Schierle, E. Weschke, A. Gienis, J. Wen, J. Schneeloch, Z. Xu, S. Ono, G. Gu, M. Le Tacon, and A. Yazdani, *Science* **343**, 393 (2014).
  - [9] J. Chang, E. Blackburn, A. T. Holmes, N. B. Christensen, J. Larsen, J. Mesot, R. Liang, D. A. Bonn, W. N. Hardy, A. Watenphul, M. v. Zimmermann, E. M. Forgan, and S. M. Hayden, *Nature Physics* **8**, 871 (2012).
  - [10] M. Hücker, N. B. Christensen, A. T. Holmes, E. Blackburn, E. M. Forgan, R. Liang, D. A. Bonn, W. N. Hardy, O. Gutowski, M. v. Zimmermann, S. M. Hayden, and J. Chang, *Phys. Rev. B* **90**, 054514 (2014).
  - [11] S. Blanco-Canosa, A. Frano, E. Schierle, J. Porras, T. Loew, M. Minola, M. Bluschke, E. Weschke, B. Keimer, and M. Le Tacon, *Phys. Rev. B* **90**, 054513 (2014).
  - [12] S. Gerber, H. Jang, H. Nojiri, S. Matsuzawa, H. Yasumura, D. A. Bonn, R. Liang, W. N. Hardy, Z. Islam, A. Mehta, S. Song, M. Sikorski, D. Stefanescu, Y. Feng, S. A. Kivelson, T. P. Devereaux, Z.-X. Shen, C.-C. Kao, W.-S. Lee, D. Zhu, and J.-S. Lee, *Science* **350**, 949 (2015).
  - [13] M.-H. Julien, *Science* **350**, 914 (2015).
  - [14] K. Fujita, M. H. Hamidian, S. D. Edkins, C. K. Kim, Y. Kohsaka, M. Azuma, M. Takano, H. Takagi, H. Eisaki, S.-i. Uchida, A. Allais, M. J. Lawler, E.-A. Kim, S. Sachdev, and J. C. S. Davis, *Proceedings of the National Academy of Sciences* **111**, E3026 (2014).
  - [15] E. Fradkin, S. A. Kivelson, and J. M. Tranquada, *Rev. Mod. Phys.* **87**, 457 (2015).
  - [16] A. Allais, J. Bauer, and S. Sachdev, *Phys. Rev. B* **90**, 155114 (2014).
  - [17] W. D. Wise, M. C. Boyer, E. Chatterjee, T. Kondo, T. Takeuchi, H. Ikuta, Y. Wang, and E. W. Hudson, *Nature Physics* **4**, 696 (2008).
  - [18] K. M. Shen, F. Ronning, D. H. Lu, F. Baumberger, N. J. C. Ingle, W. S. Lee, W. Meevasana, Y. Kohsaka, M. Azuma, M. Takano, H. Takagi, and Z.-X. Shen, *Science* **307**, 901 (2005).
  - [19] A. Amaricci, A. Camjayi, K. Haule, and G. Kotliar, *Phys. Rev. B* **82**, 155102 (2010).
  - [20] S. Sachdev and R. La Placa, *Phys. Rev. Lett.* **111**, 027202 (2013).
  - [21] P. Corboz, T. M. Rice, and M. Troyer, *Phys. Rev. Lett.* **113**, 046402 (2014).
  - [22] S. Caprara, C. Di Castro, G. Seibold, and M. Grilli, *arXiv:1604.07852 [cond-mat.supr-con]*.
  - [23] P. A. Lee, *Phys. Rev. X* **4**, 031017 (2014).
  - [24] Y. Wang, D. F. Agterberg, and A. Chubukov, *Phys. Rev. Lett.* **114**, 197001 (2015).
  - [25] W.-L. Tu and T.-K. Lee, *Scientific Reports* **6** (2016), 10.1038/srep18675.
  - [26] M. Abram, J. Kaczmarczyk, J. Jędrak, and J. Spalek, *Phys. Rev. B* **88**, 094502 (2013).
  - [27] J. Spalek, M. Zegrodnik, and J. Kaczmarczyk, *arXiv:1606.03247 [cond-mat]*.
  - [28] N. Plakida, *High-Temperature Cuprate Superconductors* (Springer, 2010) chapters 5, 7.
  - [29] R. Eder, J. van den Brink, and G. A. Sawatzky, *Phys. Rev. B* **54**, R732 (1996).
  - [30] F. C. Zhang and T. M. Rice, *Phys. Rev. B* **37**, 3759 (1988).
  - [31] F. C. Zhang, *Phys. Rev. Lett.* **90**, 207002 (2003).
  - [32] J. Jędrak, J. Kaczmarczyk, and J. Spalek, *arXiv:1008.0021 [cond-mat]*.
  - [33] J. Jędrak and J. Spalek, *Phys. Rev. B* **81**, 073108 (2010); *Phys. Rev. B* **83**, 104512 (2011).
  - [34] J. Kaczmarczyk and J. Spalek, *Phys. Rev. B* **84**, 125140 (2011); O. Howczak, J. Kaczmarczyk, and J. Spalek, *Phys. Stat. Solidi (b)* **250**, 609 (2013); A. P. Kądziaława, J. Spalek, J. Kurzyk, and W. Wójcik, *Eur. Phys. J. B* **86**, 252 (2013); M. M. Wysokiński and J. Spalek, *J. Phys.: Condens. Matter* **26**, 055601 (2014); M. M. Wysokiński, M. Abram, and J. Spalek, *Phys. Rev. B* **90**, 081114 (2014); M. Abram, *Acta Phys. Pol. A* **126**, A25 (2014); M. M. Wysokiński, M. Abram, and J. Spalek, *Phys. Rev. B* **91**, 081108 (2015); M. Abram, M. M. Wysokiński, and J. Spalek, *J. Magn. Magn. Mater.* **400**, 27 (2016).
  - [35] R. B. Laughlin, *Phil. Mag.*, 1165 (2006).
  - [36] F. Gebhard, *The Mott Metal-Insulator Transition* (Springer, 1997).
  - [37] K. A. Chao, J. Spalek, and A. M. Oles, *Journal of Physics C: Solid State Physics* **10**, L271 (1977).
  - [38] K. A. Chao, J. Spalek, and A. M. Oleś, *Phys. Rev. B* **18**, 3453 (1978).
  - [39] J. Spalek and A. M. Oleś, *Physica B+C* **86-88**, 375 (1977).

- [40] J. Spalek, A. M. Oleś, and K. A. Chao, *Phys. Status Solidi B* **87**, 625 (1978).
- [41] J. Spalek, A. M. Oleś, and K. A. Chao, *Phys. Status Solidi B* **108**, 329 (1981).
- [42] J. Spalek, *Acta. Phys. Pol. A* **111**, 409 (2007).
- [43] J. Spalek and J. M. Honig, “Metal-Insulator Transitions, Exchange Interactions, and Real Space Pairing,” (Nova Science Publishers, editor A. Narlikar, Vol. 8, 1991) pp. 1–67.
- [44] J. Spalek, *Phys. Rev. B* **37**, 533 (1988).
- [45] M. C. Gutzwiller, *Phys. Rev. Lett.* **10**, 159 (1963).
- [46] M. C. Gutzwiller, *Phys. Rev.* **137**, A1726 (1965).
- [47] J. Bünnemann, T. Schickling, and F. Gebhard, *EPL (Europhysics Letters)* **98**, 27006 (2012).
- [48] J. Kaczmarczyk, J. Spalek, T. Schickling, and J. Bünnemann, *Phys. Rev. B* **88**, 115127 (2013).
- [49] J. Kaczmarczyk, J. Bünnemann, and J. Spalek, *New Journal of Physics* **16**, 073018 (2014).
- [50] J. Kaczmarczyk, T. Schickling, and J. Bünnemann, *Phys. Status Solidi B* **252**, 2059 (2015).
- [51] M. Galassi, J. Davies, J. Theiler, B. Gough, P. Jungman, G. abd Alken, M. Booth, and F. Rossi, *GNU Scientific Library Reference Manual* (2009), 3rd ed., Network Theory, Ltd., London.
- [52] S. Tsonis, P. Kotetes, G. Varelogiannis, and P. B. Littlewood, *J. Phys.: Condens. Matter* **20**, 434234 (2008).
- [53] A. Aperis, G. Varelogiannis, and P. B. Littlewood, *Phys. Rev. Lett.* **104**, 216403 (2010).
- [54] For completeness, we have tested the influence of  $t'$  parameter. For  $t' = 0$ , while increasing the value of  $V$ , the SC dome both shrinks and moves towards  $\delta = 0$ . Therefore for  $t' = 0$ , the pure AF phase (for  $V > 0$ ) appears on the right side of the SC dome, not on the left, as it was described in the main text (for  $t' = 0.25$ ).
- [55] G. Deutscher, A. F. Santander-Syro, and N. Bontemps, *Phys. Rev. B* **72**, 092504 (2005).
- [56] C. Giannetti, F. Cilento, S. Dal Conte, G. Coslovich, G. Ferrini, H. Molegraaf, M. Raichle, R. Liang, H. Eisaki, M. Greven, A. Damascelli, D. van der Marel, and F. Parmigiani, *Nat. Commun.* **1**, 353 (2011).
- [57] H. J. A. Molegraaf, C. Presura, D. van der Marel, P. H. Kes, and M. Li, *Science* **295**, 2239 (2002).
- [58] G. Deutscher, A. F. Santander-Syro, and N. Bontemps, *Phys. Rev. B* **72**, 092504 (2005).
- [59] F. Carbone, A. B. Kuzmenko, H. J. A. Molegraaf, E. van Heumen, V. Lukovac, F. Marsiglio, D. van der Marel, K. Haule, G. Kotliar, H. Berger, S. Courjault, P. H. Kes, and M. Li, *Phys. Rev. B* **74**, 064510 (2006).
- [60] C. Giannetti, F. Cilento, S. Dal Conte, G. Coslovich, G. Ferrini, H. Molegraaf, M. Raichle, R. Liang, H. Eisaki, M. Greven, A. Damascelli, D. van der Marel, and F. Parmigiani, *Nat. Commun.* **2**, 353 (2011).
- [61] T. Ogawa, K. Kanda, and T. Matsubara, *Prog. Theor. Phys.* **53**, 614 (1975).
- [62] D. Vollhardt, *Rev. Mod. Phys.* **56**, 99 (1984).
- [63] M. Ogata and H. Fukuyama, *Reports on Progress in Physics* **71**, 036501 (2008).
- [64] B. Edegger, V. N. Muthukumar, and C. Gros, *Advances in Physics* **56**, 927 (2007).
- [65] M. M. Wysokiński, J. Kaczmarczyk, and J. Spalek, *Phys. Rev. B* **92**, 125135 (2015).